Chapter 6: Two-layer model analysis in uniform flow

6.1. Introduction

As discussed in the introduction, in fluvial hydraulics, different sets of equations are used to model the interaction between water and sediments. The most usual are the Saint-Venant – Exner equations described previously in chapter 2, where a transport layer is not explicitly considered. In this case, two closure equations have to be added to the partial differential equation system, one dealing with the friction slope (e.g. the Manning relation) and the other providing the solid discharge by any common formula (e.g. the relation proposed by Meyer-Peter–Müller, 1948).

In contrast, the two-layer approach (Capart, 2000) takes explicitly the transport layer into account. The model considers the solid discharge as a main variable, while the friction is represented by the various shear stresses at each layer interface. The solid discharge is influenced by the friction coefficients associated to those shear stresses. In uniform flow conditions, the solid discharge calculated by the two-layer model or by the common formulae should be the same, allowing to calibrate the friction coefficients.

Once calibrated for one situation (e.g. a given bottom slope), using either experimental or theoretical data, the two-layer model is able to generate the water depth and the solid discharge for any situation (e.g. other bottom slopes), without use of any transport formula. In that sense the method offers an alternative to common transport formulae.

First, analysis and comparisons are made in the case of the more complete model (Spinewine, 2005) allowing distinct velocity in each layer and taking into account the variation in sediment concentration between the bed and the transport layer. The way to calibrate the friction coefficient and the behaviour of the model in uniform flow is detailed. Then, the influence of the assumption concerning the concentration and the velocity in the transport layer is studied. In the following, the bed is assumed to be flat, without any bed forms. The results presented in this thesis are partially exposed in Savary and Zech (2006).

6.2. Two-velocity model in uniform flow conditions

The uniform steady flow takes place when the friction exactly balances the effect of gravity, inducing the bed-slope S_0 to be equal to the friction slope S_f. Moreover, in presence of sediment transport, the solid discharge is in equilibrium, showing neither erosion nor deposition. Under these conditions, there is no variation in the flow variables with time and with space. In equations (2.83-2.85), the partial derivatives with time and space are equal to zero, $\partial/\partial t = 0$ and $\partial/\partial x = 0$, except the variation of the bed level along the channel, which is defined by the equilibrium slope $\partial z_b/\partial x = -S_0$. As the sediment transport is in equilibrium, the interfaces between the bed, the transport layer and the water layer do not move, the erosion rate $e_b = 0$ and the linked z_s interface movement $e_s = 0$. These simplifications make the continuity equations (2.73) and (2.74) disappear, the momentum equations (2.76) and (2.77) are simplified to become

$$-gh_w \frac{\partial z_b}{\partial x} = gh_w S_0 = \frac{\tau_{ws}}{\rho_w} \tag{6.1}$$

$$-gh_s \frac{\partial z_b}{\partial x} = gh_s S_0 = \frac{\tau_b}{\rho_s'} - \frac{\tau_{ws}}{\rho_s'} \tag{6.2}$$

There is neither erosion nor deposition, which means that the shear stress applied on the bed τ_s has to be equal to the shear stress resisting to the flow τ_b

$$\tau_b = \tau_s \tag{6.3}$$

The unit liquid and solid discharges can be defined

$$q_w = h_w u_w \qquad q_s = C_s h_s u_s \tag{6.4a-b}$$

The expressions (2.80) to (2.82) of the various shear stresses are

$$\tau_{ws} = \rho_w C_{f,w} \left| u_w - u_s \right| \left(u_w - u_s \right) \qquad \tau_s = \rho_s' C_{f,s} \left| u_s \right| u_s$$

$$\tau_b = \tau_{crit} + tg\varphi(\rho_s' - \rho_w) g h_s \tag{6.5a-c}$$

Equations (6.1-6.4) and (6.5) form a set of 8 uniform-flow equations linking 13 parameters: S_0, q_w, q_s, h_w, h_s, u_w, u_s, τ_{ws}, τ_s, τ_b, τ_{crit}, $C_{f,w}$ and $C_{f,s}$. In uniform-flow condition, if 5 of them are known, the others may be deduced.

6.3. Friction coefficient calibration

If only 5 of the 13 parameters are imposed, measured or estimated by additional relations, it is thus possible to calibrate the two friction coefficients, $C_{f,w}$ and $C_{f,s}$.

For example, for a given discharge q_w in a channel of slope S_0 with mobile bed whose characteristic diameter is d, the water depth h_w may be deduced from any uniform-flow relation. If now the solid discharge q_s and the critical shear stress τ_{crit} are computed from any empirical formula, we obtain a set of 5 parameters (the water depth h_w, the discharges q_w and q_s, the slope S_0 and the critical shear stress τ_{crit}), required to calibrate $C_{f,w}$ and $C_{f,s}$. If experimental data are available, they can be used to find out the flow parameters h_w and q_s, in this case, existent uniform flow and solid discharge relations are no longer required.

The uniform water level corresponding to the given slope S_0 and the discharge q_w is obtained, using, for example, the Manning uniform flow relation.

$$q_w = \frac{1}{n} h_w^{5/3} S_0^{1/2} \tag{6.6}$$

where the Manning roughness coefficient n may be evaluated from the Strickler formula

$$K = \frac{1}{n} = \frac{26}{d^{1/6}} \tag{6.7}$$

The sediment discharge q_s and the critical shear stress τ_{crit}, under which no erosion is observed, are determined, for instance, with the classical formula proposed by Meyer-Peter–Müller (2.14).

$$q_s = 8\sqrt{g(s-1)d^3}\left(\left(\frac{n_b^{'}}{n_b}\right)^{3/2} \frac{\gamma_w R_b S_0}{(\gamma_s - \gamma_w)d} - 0.047\right)^{3/2} \tag{6.8}$$

$$\tau_{crit} = \tau_{crit,MPM} = 0.047(\gamma_s - \gamma_w)d \tag{6.9}$$

As bed forms are neglected, the ratio $n'_b/n_b = 1$. The uniform water depth h_w and the given slope S_0 and discharge q_w are introduced in (6.1) to calculate the shear stress applied by the water layer on the sediment transport layer τ_{ws}.

$$\tau_{ws} = \rho_w g h_w S_0 \tag{6.10}$$

The expression of the shear resistance to the flow τ_b (6.5c), is substituted in (6.2), giving an expression of h_s depending on the previously calculated shear stresses τ_{ws}, τ_{crit} and the given slope S_0.

$$h_s = \frac{\tau_{crit} - \tau_{ws}}{g(\rho_s' S_0 - (\rho_s' - \rho_w)tg\varphi)} \tag{6.11}$$

The velocity in the water layer u_w and the sediment transport layer u_s are evaluated from (6.4a-b), knowing the uniform thickness of each layer h_w and h_s and both the water discharge q_w and the sediment discharge q_s.

$$u_w = \frac{q_w}{h_w} \qquad u_s = \frac{q_s}{C_s h_s} \tag{6.12}$$

Knowing the velocity in each layer and the shear stress τ_{ws}, the expression (6.5a) allows calculating the corresponding water friction coefficient $C_{f,w}$.

$$C_{f,w} = \frac{\tau_{ws}}{\rho_w \left| u_w - u_s \right| \left(u_w - u_s \right)} \tag{6.13}$$

As the shear stress resisting to the flow τ_b (6.5c), is equal to the shear stress applied to the bed τ_s (6.5b), the sediment friction coefficient $C_{f,s}$ can be isolated in (6.5b).

$$C_{f,s} = \frac{\tau_s}{\rho_s' \left| u_s \right| u_s} = \frac{\tau_b}{\rho_s' \left| u_s \right| u_s} \tag{6.14}$$

These two friction coefficients are obtained for a specific flow, characterised by given water discharge and bed slope corresponding to a water Froude number. They can be calculated, by the same method, for various Froude numbers.

An example was computed with the following data: a unit water discharge q_w taking the value of 0,1 m³/s, 1 m^3/s/m and 10 m^3/s/m in a channel whose bed is constituted of uniform grains of diameter $d = 1$ mm; the density $s = \rho_s/\rho_w = 2.65$, and the repose angle of the soil $\varphi = 30°$.

The calculated friction coefficients are presented in Figures 6.1 and 6.2, each curve is related to a water discharge, they are computed for a range of bed-slopes corresponding to a range of Froude numbers in abscissa.

The calibration value of the coefficients varies with the Froude number, in order to perfectly match the Manning and Meyer-Peter–Müller formulations. However, in the numerical model, the coefficients have to remain constant during the computation, even if the modelled flow does not correspond to a unique Froude number. Then, the coefficients are calibrated on the average expected Froude number, implying the two-layer model is not totally equivalent to the Manning and Meyer-Peter–Müller relations for other Froude numbers.

As illustrated in Figure 6.2, the calibration value of $C_{f,s}$ does not vary a lot with the Froude number. It implies that the two-layer model, based on an unique value of $C_{f,s}$, is not too different from the Meyer-Peter–Müller approach. On the other hand, the calibration value of $C_{f,w}$ is quite variable with the Froude number, revealing that the model does not follow the friction law proposed by Manning. This last observation was predictable looking at the expressions of the shear stresses (6.5a-b), which are Chézy-like expressions.

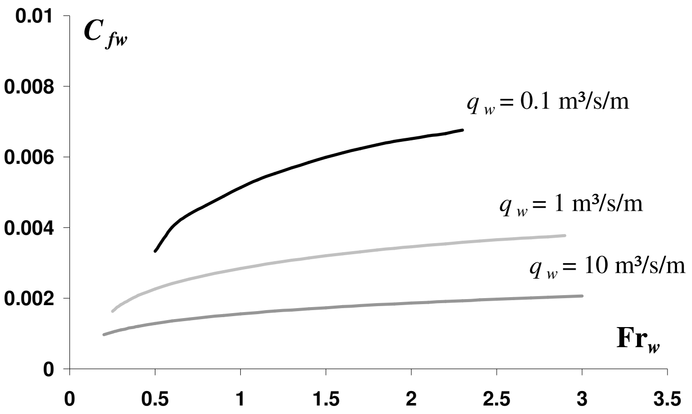

Figure 6.1. Evolution of the calibrated friction coefficients $C_{f,w}$ (calibrated with Manning) with Froude number Fr_w (d = 1 to 10 mm)

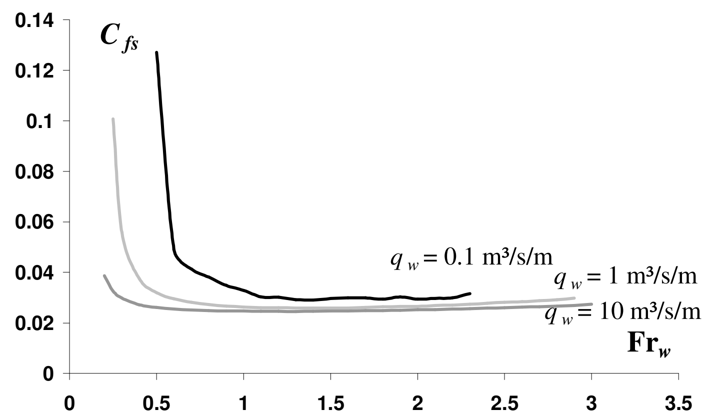

Figure 6.2. Evolution of the calibrated friction coefficients $C_{f,s}$ (calibrated with Manning) with Froude number Fr_w (d = 1 to 10 mm)

The Manning formula in the calibration process (6.6) could be replaced by the Chézy uniform flow relation

$$q_w = C h_w^{3/2} S_0^{1/2} \tag{6.15}$$

where C is the Chézy friction coefficient assumed to be constant, depending only of the bed material. This relation is different from the Manning formulation, which links the Chézy friction coefficient to the hydraulic radius ($R = h_w$, in the case of unit width)

$$C = \frac{1}{n} h_w^{1/6} \tag{6.16}$$

If the Chézy expression is used to deduce the uniform depth, the calibration values of the friction coefficients $C_{f,w}$ and $C_{f,s}$ are computed for the previous example and plotted in Figures 6.3 and 6.4.

The calibration values of $C_{f,s}$ are not significantly modified (Fig. 6.4) and the calibration values of $C_{f,w}$ become less dependent of the Froude number. This confirms that the two-layer model is closer to the friction law proposed by Chézy than to the one proposed by Manning. Moreover it reveals that $C_{f,w}$ is linked to the friction, while $C_{f,s}$ is mainly related to the sediment transport.

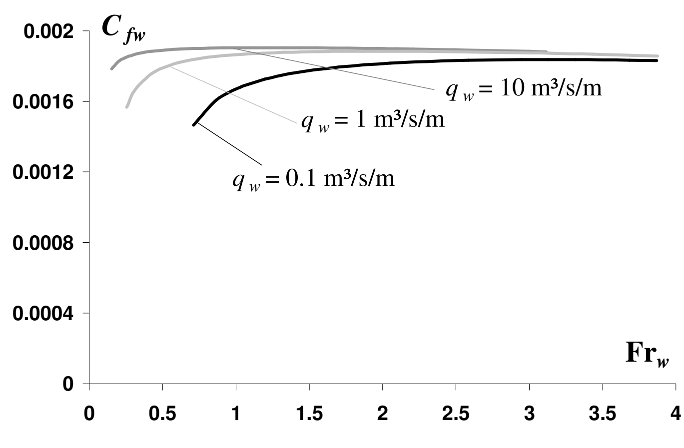

Figure 6.3. Evolution of the calibrated friction coefficients $C_{f,w}$ (calibrated with Chézy) with Froude number Fr_w (d = 1 to 10 mm)

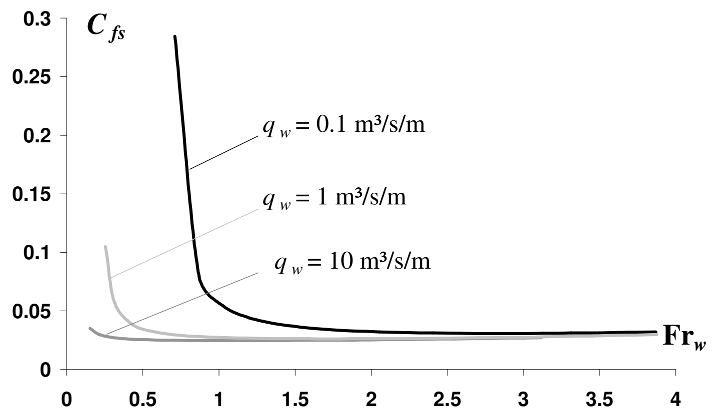

Figure 6.4. Evolution of the calibrated friction coefficients $C_{f,s}$ (calibrated with Chézy) with Froude number Fr_w (d = 1 to 10 mm) ($q_w = 10\ \mathrm{m^3/s/m}$)

In all cases, for too low sediment transport, the calibration values of both coefficients change a lot, the solid transport formula used for the calibration being not appropriate anymore.

6.4. Two-velocity model behaviour

Once the friction coefficients $C_{f,w}$ and $C_{f,s}$ are calibrated for a specific Froude number, one may investigate the behaviour of the two-layer model under other flow conditions by considering various combinations of q_w and S_0. For each combination, it is possible to compute q_s, h_w, h_s, u_w, u_s, τ_{crit}, τ_{ws}, τ_s and τ_b., only using the relations (6.1) to (6.5) and the Meyer-Peter–Müller proposal for τ_{crit} (6.9).

To analyse the two-layer model behaviour, the example treated below (Figs. 6.5 to 6.13) was computed with the following data: the unit water discharge $q_w = 10\ \mathrm{m^3/s/m}$ in a channel whose bed is constituted of uniform grains of diameter d varying from 1 to 10 mm; the density $s = \rho_s/\rho_w = 2.65$, and the repose angle of the soil $\varphi = 30°$.

For each diameter, the calibration of $C_{f,w}$ and $C_{f,s}$ is done for a bottom slope S_0 corresponding to the value of the Froude number $\mathrm{Fr}_w = 2$. Then, for each diameter, a range of bottom slopes is explored. Using the set of equations

(6.1) to (6.5) and (6.9), it is possible to compute the various parameters depending on the Froude number.

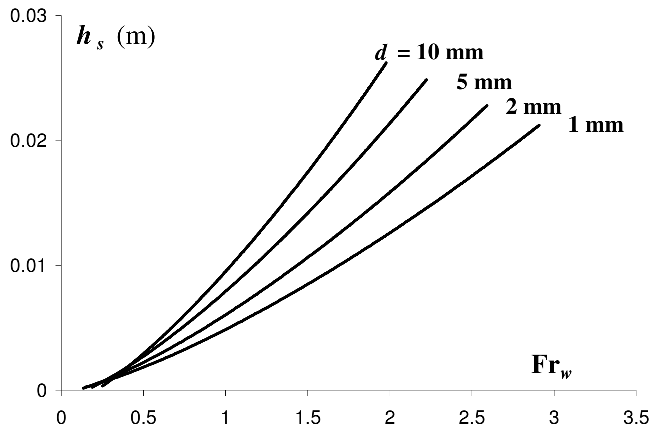

Figure 6.5. Evolution of the sediment-layer depth h_s (computed with the two-layer model) with Froude number Fr_w (d = 1 to 10 mm) (q_w = 10 m^3/s/m)

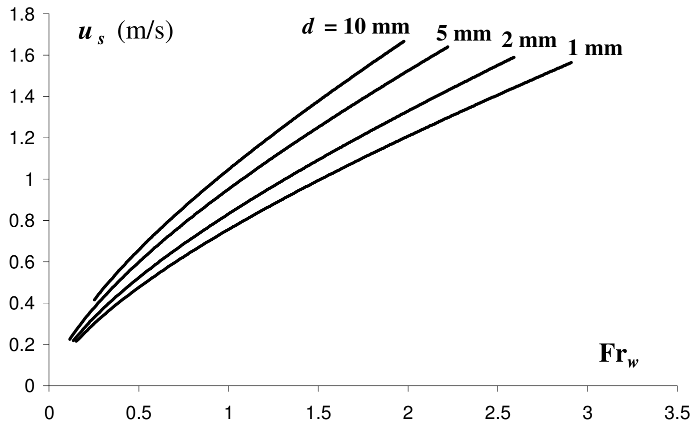

Figure 6.6. Evolution of the sediment-layer velocity u_s (computed with the two-layer model) with Froude number Fr_w (d = 1 to 10 mm) (q_w = 10 m^3/s/m)

From Figures 6.5 and 6.6, it clearly appears that as well the sediment-layer depth h_s as its velocity u_s increase with increasing Froude number (thus with increasing bottom slope S_0, decreasing water depth h_w, and increasing water velocity u_w). The resulting raise of solid discharge q_s is due, for a part, to the increase of the transport layer velocity u_s, but mainly to the development in depth of the sediment layer h_s.

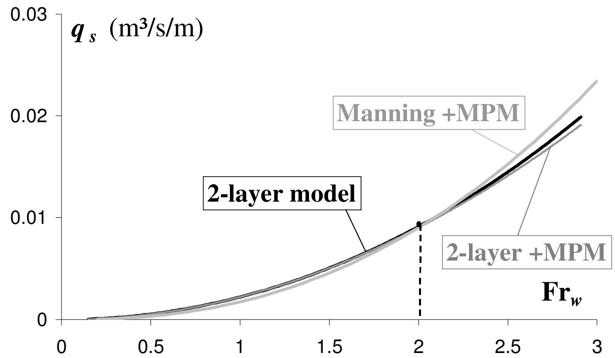

Figure 6.7. Evolution of solid discharge q_s with Froude number Fr_w : comparison between two-layer model and Meyer-Peter–Müller formula (d = 1 mm, q_w = 10 m^3/s/m, $C_{f,w}$ = 0.0016, $C_{f,s}$ = 0.069)

Computing the solid discharge from (6.4b) yields a result very close to the Meyer-Peter–Müller formula (Fig. 6.7). The latter formula was used to calibrate the two-layer model for $Fr_w = 2$. The three curves in Figure 6.7 represent three ways to compute q_s for other Froude numbers. One is calculated with the two-layer model, another is obtained applying Meyer-Peter–Müller formula to the water depth h_w calculated with the two-layer model and the last is calculated completely independently with Manning and Meyer-Peter–Müller formulae. That means that the two-layer model and its closure equations (6.1-6.5) are at least consistent with the predictions of Meyer-Peter and Müller. As the curves on Figure 6.7 are quite close, the value of Froude number chosen to calibrate the friction coefficients is not very important. This confirms the conclusion issued from Fig 6.2 and 6.4 showing that the calibration value of $C_{f,s}$ does not vary a lot with the Froude number. This consistency is confirmed for other grain diameters (d = 2, 5 and 10 mm) and other unit discharges (q_w = 1 m^3/s/m and 0.1 m^3/s/m), at least if the calibration conditions are not too close to the threshold τ_{crit} under which no transport is expected.

As shown in Figure 6.8, there can be large differences between the sediment transport rates estimated by different semi empirical physical models. It seems that the two-layer model can reproduce several of these classical formulations, provided that the right combination of $C_{f,w}$ and $C_{f,s}$ is imposed.

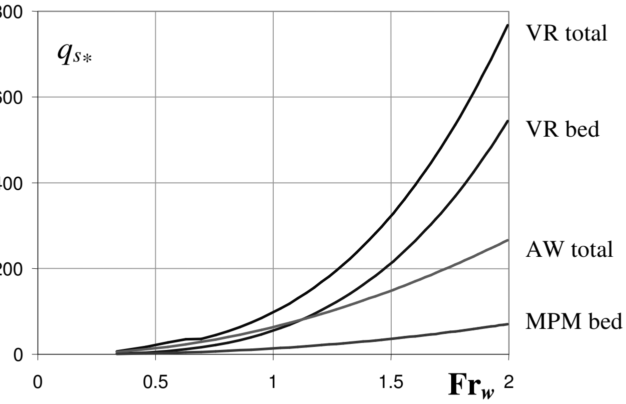

Figure 6.8. Dimensionless solid discharge in uniform flow conditions - d = 1 mm; q = 10 m^3/s/m; VR = van Rijn formula (bed load and total load), AW = Ackers-White formula (total load), MPM = Meyer-Peter–Müller formula (bed load). Zech et al. (2005)

The Meyer-Peter–Muller relation (6.8) used to estimate the solid discharge, in the calibration process, could be replaced by another sediment transport formula like the one proposed by Ackers-White (1980) for example. The calibrated values of the friction coefficients $C_{f,s}$ and $C_{f,w}$ depend on the estimation of the solid discharge, which depends in turn on the sediment transport formula used.

If the Ackers-White formula is used instead of the Meyer-Peter–Muller formula in the previous example (q_w = 10 m^3/s/m, d = 1 mm; $\rho_s/\rho_w = 2.65$, $\varphi = 30°$, $\mathrm{Fr}_w = 2$), the obtained frictions parameters are significantly different. The calibrated friction coefficients obtained on the basis of the Meyer-Peter–Müller formula are $C_{f,w} = 0.0018$ and $C_{f,s} = 0.025$, while they become $C_{f,w} = 0.0088$ and $C_{f,s} = 0.0017$ when the Ackers-White formula is used. The solid discharge calculated by the two-layer model is compared with the formulae of Meyer-Peter–Müller and Ackers-White in Figure 6.9. Each computation is in good agreement with the corresponding formula. As the parameters $C_{f,s}$ and $C_{f,w}$ depend significantly on the chosen formula, it is important to select a formula whose range of application corresponds to the problem.

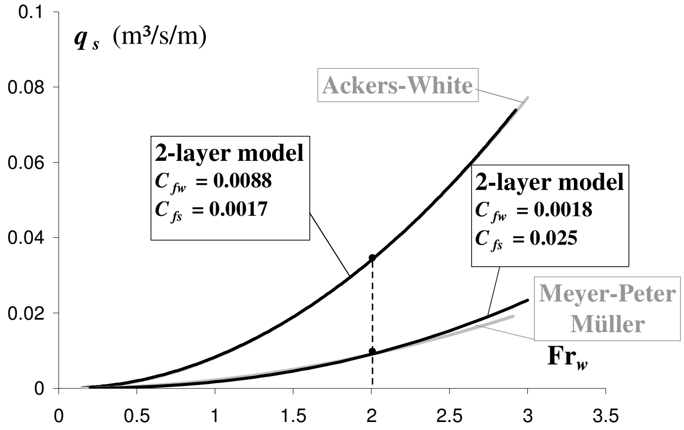

Figure 6.9. Solid discharge: comparison between two-layer model, Meyer-Peter–Müller formula and Ackers White formula (d = 1 mm, τ_{crit} = 0.76 N/m^2, q_w = 10 m^3/s/m, $C_{f,w}$ = 0.0016 / 0.0032, $C_{f,s}$ = 0.069 / 0.0049)

Figures 6.10 and 6.11 illustrate the way the friction coefficients $C_{f,w}$ and $C_{f,s}$ evolve depending on the sediment diameter d and the water discharge q_w. Actually, these figures indicate which calibration value should be chosen for the friction coefficients knowing only few flow parameters (the grain diameter d and the water discharge q_w). The two coefficients seem to increase with the diameter d and to decrease with the water discharge q_w. In these figures, the coefficients are calibrated with one specific sediment transport formula for a single Froude number. The important raise of $C_{f,s}$ with the diameter for the smallest water discharge (q_w = 0.1 m³/s) is due to the proximity of the sediment transport threshold. If the grain diameter d is too important and the discharge q_w is too low, the sediment transport is close to zero and the formula used for the calibration is out of its application range.

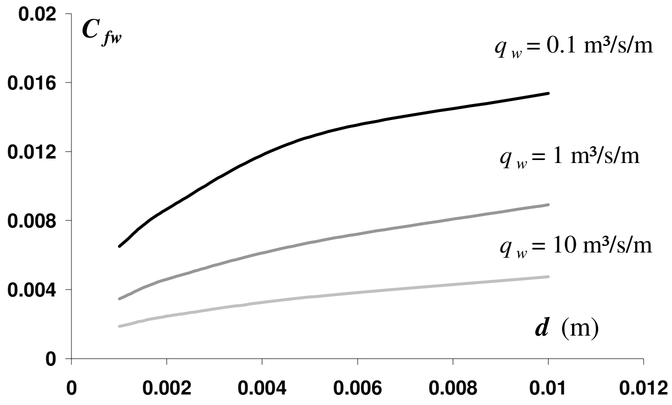

Figure 6.10. Evolution of the friction coefficient $C_{f,w}$ with grain diameter d and water discharge q_w (calibration based on the Meyer-Peter–Müller formula, $\mathrm{Fr}_w = 2$).

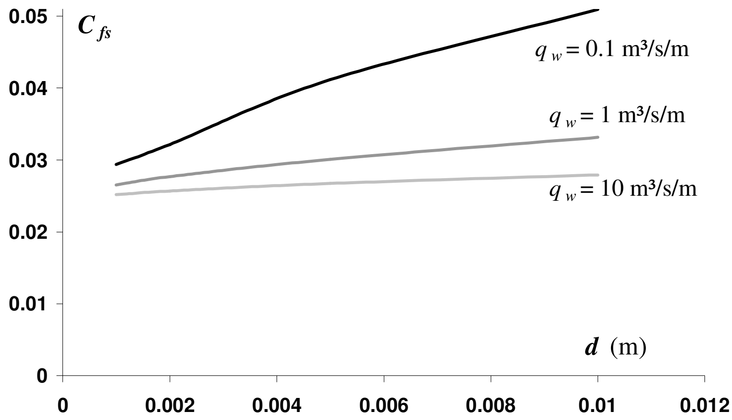

Figure 6.11. Evolution of the friction coefficient $C_{f,s}$ with grain diameter d and water discharge q_w (calibration based on the Meyer-Peter–Müller formula, $\mathrm{Fr}_w = 2$)

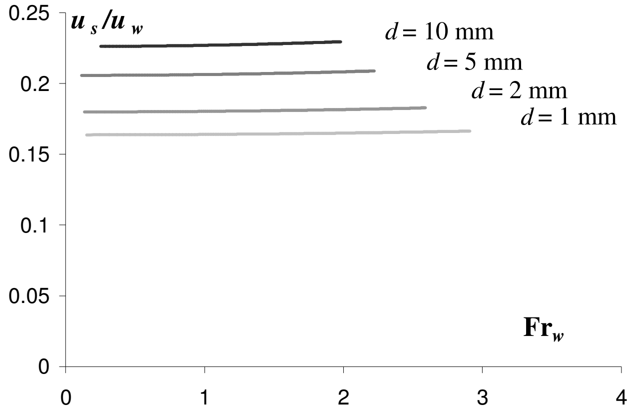

Figure 6.12. Evolution of the ratio of velocity u_s/u_w in each layer with Froude number Fr_w (calibration based on the Meyer-Peter–Müller formula, $\mathrm{Fr}_w = 2$)

For a given ρ_s, the ratio between the velocity in each layer u_s/u_w is quite constant with the water Froude number (Fig. 6.12), it only depends on the diameter and the water discharge (Fig. 6.13). The velocity ratio decreases with the discharge and increases with the diameter to reach asymptotically a near steady value.

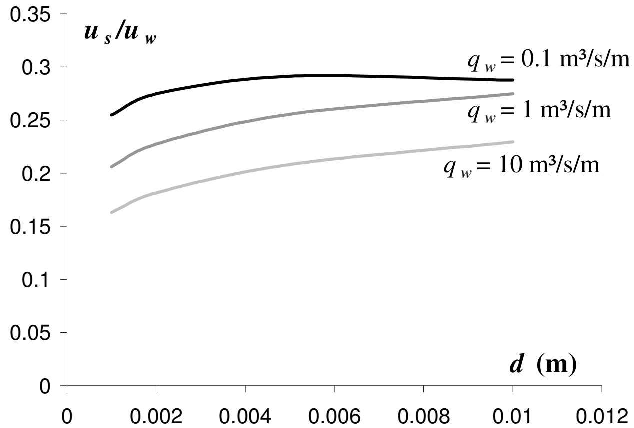

Figure 6.13. Evolution of the ratio of velocity u_s/u_w in each layer with grain diameter d and water discharge q_w (calibration based on the Meyer-Peter–Müller formula, $\mathrm{Fr}_w = 2$)

6.5. Equivalent sediment equilibrium transport formula

Once the friction coefficients are calibrated, a solid discharge formulation corresponding to the two-layer model in equilibrium state can be deduced. For a known uniform water depth h_w, the expressions of the transport layer thickness h_s and velocity u_s can be substituted in (6.4b). The sediment transport thickness h_s can be expressed by (6.11) in which the formulation of the water shear stress τ_{ws} (6.10) is introduced.

$$h_s = \frac{\tau_{crit} - \rho_w g h_w S_0}{g\left(\rho_s' S_0 - (\rho_s' - \rho_w) tg\varphi\right)} = \frac{\rho_w g h_w S_0 - \tau_{crit}}{g\left(\rho_s'(tg\varphi - S_0) - \rho_w tg\varphi\right)} \quad (6.17)$$

If the bed slope S_0 is negligible when compared to $tg\varphi$, which is equal to 0.577 for a soil repose angle of 30°, the expression of h_s is simplified.

$$h_s = \frac{\rho_w g h_w S_0 - \tau_{crit}}{g(\rho_s' - \rho_w) tg\varphi} \quad (6.18)$$

The expression of the velocity u_s can be deduced by expressing that the applied shear stress τ_s (6.5b) is equal to the shear stress resisting to the flow τ_b (6.5c), where h_s (6.18) is introduced.

$$u_s = \sqrt{\frac{1}{\rho_s' C_{f,s}}\left(g(\rho_s' - \rho_w) tg\varphi \frac{\rho_w g h_w S_0 - \tau_{crit}}{g(\rho_s' - \rho_w) tg\varphi} + \tau_{crit}\right)} = \sqrt{\frac{\rho_w g h_w S_0}{\rho_s' C_{f,s}}} \quad (6.19)$$

The solid discharge is obtained from (6.4b), where (6.18) and (6.19) are substituted.

$$q_s = \frac{C_s}{\sqrt{\rho_s' C_{f,s}}\, g(\rho_s' - \rho_w) tg\varphi}\left(\rho_w g h_w S_0 - \tau_{crit}\right)\sqrt{\rho_w g h_w S_0} \quad (6.20)$$

For important Froude numbers, corresponding to important bed slopes, if the critical shear stress, representing the erosion threshold is neglected, an approximated expression for the solid discharge becomes

$$q_s = \frac{C_s}{\sqrt{\rho_s' C_{f,s}}\, g(\rho_s' - \rho_w) tg\varphi} (\rho_w g h_w S_0)^{3/2} \tag{6.21}$$

The Meyer-Peter-Muller formula, when the critical shear stress is neglected, yields

$$q_s = \frac{8\sqrt{gd^3(\rho_s - \rho_w)/\rho_w}}{\sqrt{(\rho_s - \rho_w)^3 g^3 d^3}} (\rho_w g h_w S_0)^{3/2} = \frac{8}{g(\rho_s - \rho_w)\sqrt{\rho_w}} (\rho_w g h_w S_0)^{3/2} \tag{6.22}$$

If the two-layer solid discharge (6.21) is confronted with the Meyer-Peter–Müller solid discharge (6.22), an approximate value of the sediment friction coefficient is

$$C_{f,s} = \frac{\rho_w}{\rho_s'} \left(\frac{1}{8tg\varphi} \frac{(\rho_s - \rho_w)}{(\rho_s' - \rho_w)} C_s \right)^2 = \frac{\rho_w}{\rho_s'} \left(\frac{1}{8tg\varphi} \right)^2 \tag{6.23}$$

This expression gives only an approximated value of the friction coefficient $C_{f,s}$, under the following assumptions (these assumptions arose from a discussion with Benoit Spinewine).

$$S_0 << tg\varphi \qquad\qquad \tau_{crit} << \rho_w g h_w S_0 \tag{6.24a-b}$$

Even if the bed-slope increases for high Froude numbers, the assumption (6.24a) is quite well verified ($tg\varphi = 0.577$ for a soil repose angle φ of 30°). However, for small Froude numbers, not far from the transport threshold, the critical shear stress is not negligible in comparison to the applied shear stress and the assumption (6.24b) is no longer valid.

This approximate formula (6.21) can be applied to the example treated above, where the soil repose angle is 30° and the volumetric mass of the transport layer ρ_s' is 1990 kg/m³ (corresponding to a concentration in sediment C_s of 0.6). The approximate calibration friction coefficient $C_{f,s} = 0.247$ calculated by (6.23), is confronted with the exact calibration values plotted in Figure 6.2. The estimation corresponds to a minimum value close to the value obtained for an intermediate Froude number, far from the threshold of sediment transport and from too important slopes. The approximated value of the sediment friction coefficient does not depend on the grain diameter, although the exact value changes when the grain diameter changes. The reason is that the effect of the grain diameter is entirely introduced in the critical shear stress, which is not taken into account in the approximated value (6.23).

If the simplified expression of the velocity in the transport layer u_s (6.19) is substituted in the relation (6.5a), which is itself introduced in (6.1), a simplified expression of the velocity in the water layer can be deduced.

$$u_w = \sqrt{g h_w S_0}\left(\sqrt{\frac{\rho_w}{\rho_s' C_{f,s}}} + \sqrt{\frac{1}{C_{f,w}}}\right) \tag{6.25}$$

Then, considering expressions (6.19) and (6.25), the ratio between the velocity in the two layers is

$$\frac{u_s}{u_w} = \frac{\sqrt{\rho_w C_{f,w}}}{\sqrt{\rho_w C_{f,w}} + \sqrt{\rho_s' C_{f,s}}} \tag{6.26}$$

It implies that the velocity ratio is constant, if the bed slope S_0 is negligible in comparison with $tg\varphi$. This observation is in agreement with Figure 6.12, revealing a quasi-constant ratio for varying Froude numbers.

6.6. Influence of concentration in sediment in the transport layer

The two models (equal versus distinct concentrations) adopt the same reduced form in uniform flow (6.1) to (6.5). The only difference is the value of the sediment concentration C_s and the induced volumetric mass ρ_s’ in the transport layer. In the model assuming identical concentrations, the concentration of the transport layer is set to 0.6 as in the fixed bed, while in the distinct-concentration model, the concentration of the transport layer is set to 0.22, according to Sumer et al. (1996) results.

The parameters are calibrated for $\mathrm{Fr}_w = 2$. For the one- and the two-concentration model, $C_{f,w}$ was found nearly identical $C_{f,w} = 0.00187$ (one-concentration) vs. $C_{f,w} = 0.00185$ (two-concentration), while $C_{f,s}$, is significantly distinct $C_{f,s} = 0.025$ (one-concentration) vs. $C_{f,s} = 0.038$ (two-concentration).

Unsurprisingly, the transport layer thickness (Fig. 6.14) is a little more than $0.6 / 0.22 \approx 3$ times higher in the two-concentration model when the concentration is 0.22 instead of 0.6 in the transport layer. The velocity in the transport layer (Fig. 6.15) decreases a little in the two-concentration model. The difference in concentration influences mainly the depth of the transport layer. The solid discharge (Fig. 6.16) remains close to Meyer-Peter–Müller predictions for both models, revealing that the effect on the solid discharge of a change in concentration is negligible.

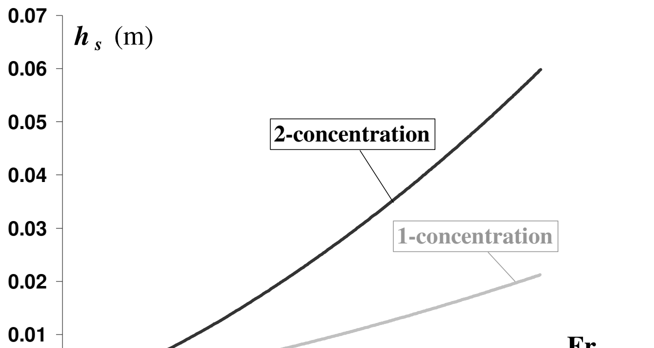

Figure 6.14. Evolution of the sediment-layer depth h_s with Froude number Fr_w : comparison between the one-concentration model (concentration of the transport layer = 0.6) and the two-concentration model (concentration of the transport layer = 0.2) (d = 1 mm, q_w = 10 m^3/s/m)

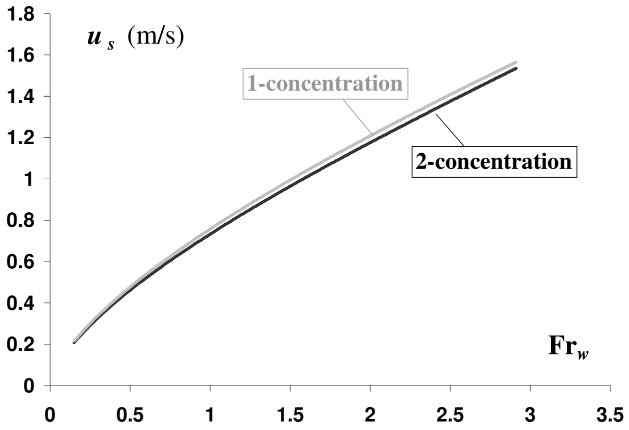

Figure 6.15. Evolution of the sediment-layer velocity u_s with Froude number Fr_w : comparison between the one-concentration model (concentration of the transport layer = 0.6) and the two-concentration model (concentration of the transport layer = 0.2) (d = 1 mm, q_w = 10 m^3/s/m)

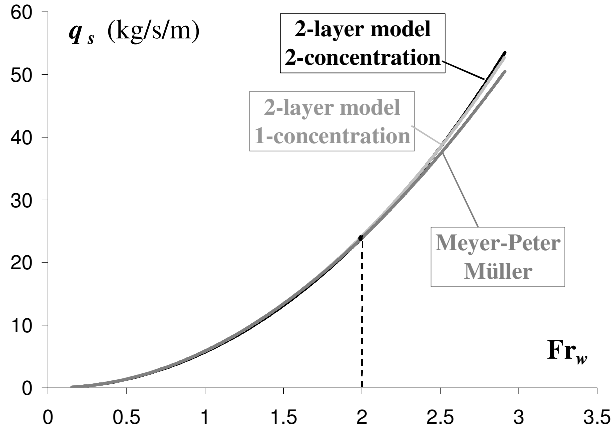

Figure 6.16. Evolution of sediment transport q_s with Froude number Fr_w comparison between the one-concentration model (concentration of the transport layer = 0.6), the two-concentration model (concentration of the transport layer = 0.2) and the Meyer-Peter–Müller formula (d = 1 mm, q_w = 10 m^3/s/m)

6.7. Influence of the assumption concerning the velocity in the transport layer

6.7.1. One-velocity model

The two-layer equations developed in the case of identical velocity in the water layer and in the transport layer (Capart 2000, Fraccarollo et al. 2003) (2.106-2.109) are simplified in uniform flow conditions. The partial derivatives with time and space are equal to zero, $\partial/\partial t = 0$ and $\partial/\partial x = 0$, except the slope $\partial z_b/\partial x = -S_0$. As the sediment transport is in equilibrium, the bed level does not move, implying the erosion rate $e_b = 0$. These simplifications make the continuity equations (2.106) and (2.107) disappear and the momentum equation (2.109) simplify to become

$$-g\frac{\partial z_b}{\partial x} = -gS_0 = \frac{-\tau_m}{\rho_w\left(h_m + rh_s\right)} \tag{6.27}$$

where the total depth is $h_m = h_w + h_s$ (6.28)

The sediment transport is in equilibrium, which means that neither erosion nor deposition occurs; thus the definition of the erosion rate e_b (2.108), which is equal to zero, is reduced to the condition

$$\tau_b = \tau_m \tag{6.29}$$

The unit total (liquid and solid) and solid discharges can be defined

$$q_m = q_w + q_s = h_m u_m \qquad q_s = Ch_s u_m \tag{6.30a-b}$$

The expressions (2.111) and (2.112) of the various shear stresses are

$$\tau_m = \rho_m Cf_m \left|u_m\right| u_m \qquad \tau_b = \tau_{crit} + tg\varphi(\rho_s' - \rho_w)gh_s \tag{6.31a-b}$$

Equations (6.27-6.31) form a set of 7 uniform-flow equations linking 11 parameters: S_0, q_m, q_s, h_m, h_w, h_s, u_m, τ_m, τ_b, $C_{f,m}$ and τ_{crit}.

Since the flow is uniform, if 4 of the parameters are known, the others may be deduced. For a given bed slope S_0, and a given water discharge q_w, the water level h_w is the uniform depth calculated with a uniform flow friction formula like Manning. Knowing the water depth and the equilibrium slope, it is possible to calculate the corresponding solid discharge with a common solid transport formula, Meyer-Peter–Müller for instance. The total discharge is obtained by adding the known water discharge and sediment discharge. The other 7 parameters are evaluated by an iterative method using relations (6.27-6.31). As the water depth and discharge are known, the velocity in the water layer and the identical mean velocity u_m are deduced. Once u_m is calculated, h_s is evaluated with (6.30b)

$$h_s = \frac{q_s}{C\, u_m} \tag{6.32}$$

The total depth h_m is the addition of each previously calculated layer thickness. Then, the friction coefficient $C_{f,m}$ is isolated in expression (6.31a)

$$C_{f,m} = \frac{\rho_w g\left(h_m + r h_s\right) S_0}{\rho_m u_m \left|u_m\right|} \tag{6.33}$$

The calibration value of the critical shear stress can be calculated by equalling the applied shear stress τ_m and the resistant shear stress τ_b (6.29). In opposition to the two-velocity model, only one friction coefficient $C_{f,m}$ remains. The critical shear stress τ_{crit} has to be calibrated in the same way as the friction coefficient, if it was estimated with an external expression (Meyer-Peter–Müller for example), the problem would be over-determinate and no solution would exist.

The friction coefficient $C_{f,m}$ and the resistant shear stress τ_{crit} are calibrated for specific flow conditions. The variation of these parameters with the flow conditions is analysed through an example computed with the following data: a unit water discharge q_w of 10 m^3/s/m in a channel whose bed is constituted of uniform grains of diameter d of 1 mm; the density $s = \rho_s/\rho_w = 2.65$, and the repose angle of the soil $\varphi = 30°$. The calibrated values are calculated for various slopes S_0 corresponding to various Froude numbers. The results are plotted in Figure 6.17 for $C_{f,m}$ and in Figure 6.18 for τ_{crit}.

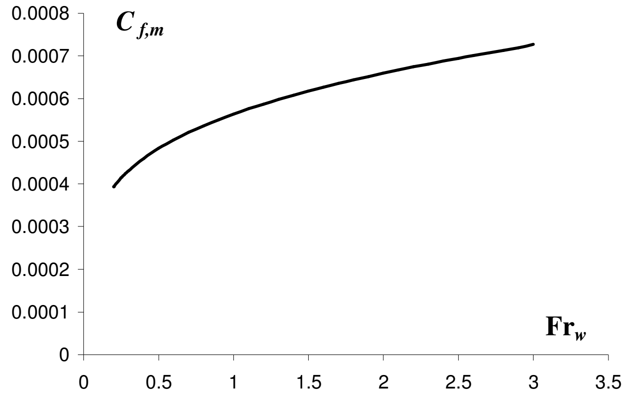

Figure 6.17. What should be the variation of coefficient $C_{f,m}$ with Froude number Fr_w to make the one-velocity model match Meyer-Peter–Müller (d = 1 mm, q_w = 10 m^3/s/m)

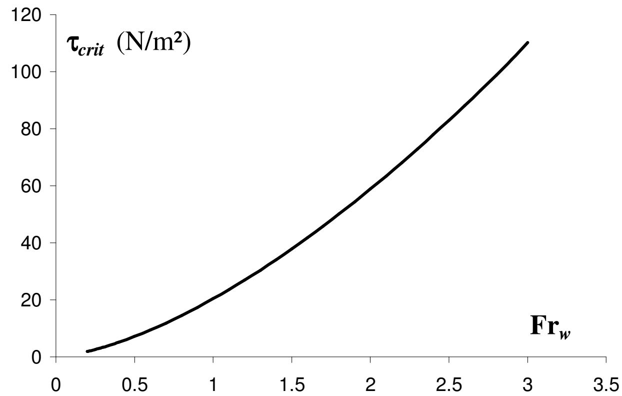

Figure 6.18. What should be the variation of critical shear stress $\tau_{m,\ crit}$ with Froude number Fr_w to make the one-velocity model match Meyer-Peter–Müller (d = 1 mm, q_w = 10 m^3/s/m)

Figures 6.17 and 6.18 illustrate how the parameters $C_{f,m}$ and τ_{crit} should vary with Froude number (instead of being constant) to match the Meyer-Peter–Müller and the Manning formulae.

As it was the case for $C_{f,w}$ in the two-velocity model, the variation of the friction coefficient $C_{f,m}$ with the water Froude number illustrates the difference between Manning and Chézy formulations. The Manning formula is used for the calibration, while the expression (6.31a), used in the two-layer model, is Chézy-like. According to the formula of Meyer-Peter–Müller, the shear stress applied to the bed τ_m is expressed

$$\tau_{m,MPM} = \gamma_m R_b S_0 = \gamma_m h_m S_0 , \tag{6.34}$$

which becomes using the Manning formulation

$$\tau_{m,MPM} = \gamma_m n^2 \frac{u_m^2}{h_m^{1/3}} = \alpha \frac{u_m^2}{h_m^{1/3}} \tag{6.35}$$

where α is a constant and n the constant Manning friction coefficient, or using the Chézy formulation

$$\tau_{m,MPM} = \gamma_m \frac{1}{C_f^2} u_m^2 = \beta u_m^2 \tag{6.36}$$

where β is a constant and C_f the constant Chézy friction coefficient. If the expression of τ_m in the two-layer model is compared to the relation based on Manning (6.35) and Chézy (6.36), the friction coefficient $C_{f,m}$ would be respectively

$$C_{f,m} = \frac{gn^2}{h_m^{1/3}} \tag{6.37}$$

$$C_{f,m} = \frac{g}{C_f^2} \tag{6.38}$$

The variation observed in Figure 6.17 is due to the difference between these expressions. The solution to obtain a constant coefficient $C_{f,m}$ would be to unify the calculation of the shear stress applied to the bed both in the model and in the calibration, as exposed for the two-velocity model.

However, the main problem remains the important variation of the critical shear stress with the Froude number. Instead of being constant, the critical shear stress rises sharply with the increasing Froude number (Fig. 6.18). As the critical shear stress is set constant, the resistant shear stress τ_b is underestimated for high Froude number inducing too much transport and overestimated for low Froude number. An artificial correction of the critical shear stress depending on the Froude number would allow the model to fit better with the classical formulation of sediment transport as the one proposed by Meyer-Peter–Müller. The variability of the critical shear stress underlines the fact that the expression of the shear stress τ_b (6.31b) is not appropriate under the assumption of identical velocity in both layers. The values of the critical shear stress deduced from the calibration point cannot be extended to other flow conditions

The calibration of $C_{f,m}$ and τ_{crit} was done for a bottom slope S_0 corresponding to the value of the Froude number $\mathrm{Fr}_w = 2$ for a water discharge of 10 m³/s/m and a grain diameter of 1 mm. During the calibration stage, the water depth h_w was estimated with Manning relation and the corresponding sediment transport q_s was evaluated with Meyer-Peter–Müller formula. The solid discharge computed from equations (6.27-6.31) with the calibrated friction coefficient $C_{f,m}$ and critical shear stress τ_{crit} is compared with the Meyer-Peter–Müller formula and the two-velocity model results in Figure 6.19.

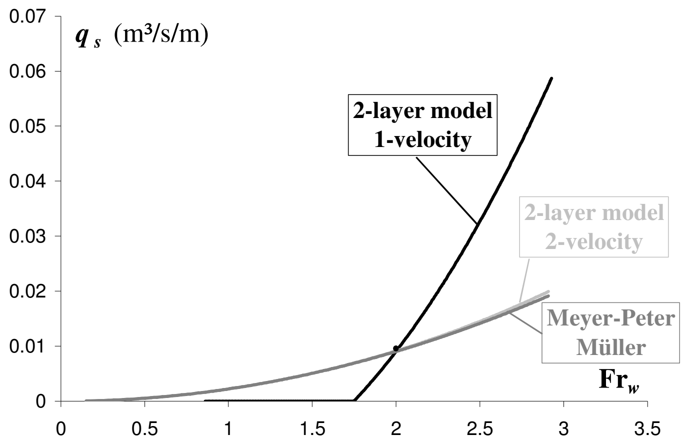

Figure 6.19. Evolution of sediment transport q_s with Froude number Fr_w comparison between the one-velocity model, the two-velocity mode and Meyer-Peter–Müller formula (d = 1 mm, q_w = 10 m^3/s/m)

In case of $\mathrm{Fr}_w > 2$, the computed solid discharge highly overestimates the solid discharge calculated by the Meyer-Peter–Müller formula. While in case of $\mathrm{Fr}_w < 2$, the computed solid discharge underestimates the Meyer-Peter–Müller formula, too quickly reaching zero with decreasing Froude number. The only Froude number for which the two ways to calculate the solid discharge are identical is $\mathrm{Fr}_w = 2$ corresponding to the calibration point. In opposition with the previous models, no match with the classical formulae is observed for constant parameters $C_{f,m}$ and τ_{crit}.

The velocity in the sediment layer $u_s = u_m$ is overestimated (close to u_w), thus for a given solid discharge the thickness of the transport layer h_s is underestimated. According to (6.31a) and (6.31b), the shear stress applied to the bed τ_m is overestimated and the part of the shear stress resisting to the flow τ_b linked to h_s is underestimated. In equilibrium conditions, these two shear stresses have to be equal (6.29). The deduced critical shear stress τ_{crit} is excessive in comparison with the one proposed by Meyer-Peter–Müller. It explains why the one-velocity model reaches the sediment motion threshold for higher Froude number than the one predicted by Meyer-Peter–Müller. The inappropriate estimation of the shear stresses also explains the overestimation in sediment transport for high Froude numbers. This implies that the one-velocity model is not able to correctly approach non-uniform flow. Then, it illustrates the relevance of allowing the velocity in the sediment transport layer to be distinct from the velocity in the water layer.

6.7.2. Two-velocity constant velocity ratio model

The adapted two-velocity model (2.100-2.102) assumes the ratio between the velocity in the water layer and the velocity in the sediment transport layer $\alpha = u_s / u_w$ is a constant. This assumption revealed to be appropriate as for constant friction coefficients this ratio remains constant, not depending on the Froude number (Fig. 6.12). Like the friction coefficients, this ratio should be calibrated.

Under uniform flow conditions, the momentum equation simplifies

$$g(\rho_w h_w + \rho_s' h_s)\frac{\partial z_b}{\partial x} = g h_s S_0 = -\tau_b \tag{6.39}$$

The liquid and solid discharges are

$$q_w = h_w u_w \qquad q_s = \alpha C_s h_s u_w \tag{6.40a-b}$$

The shear stresses (2.99) and (2.82) are equal in equilibrium conditions

$$\tau_b = \tau_s \tag{6.41}$$

where

$$\tau_s = \alpha^2 \rho_s' C_{f,s} |u_w|\, u_w \quad \text{and} \quad \tau_b = \tau_{crit} + tg\varphi(\rho_s' - \rho_w) g h_s \tag{6.42a-b}$$

Equations (6.39) to (6.42) form a set of 6 uniform-flow equations linking 11 parameters: S_0, q_w, q_s, h_w, h_s, u_w, τ_s, τ_b, τ_{crit}, α and $C_{f,s}$. In uniform-flow condition, if 5 of them are known, the others may be deduced. As it was the case for the two-velocity model, for a given water discharge and bed slope, the water depth can be calculated with the Manning uniform flow formula (6.6) and the solid discharge and critical shear stress with the Meyer-Peter–Müller formula (6.8). Then, introducing (6.42) in (6.39), it is possible to find h_s

$$h_s = \frac{\tau_{crit} - \rho_w g h_w S_0}{g(\rho_s' S_0 - (\rho_s' - \rho_w) tg\varphi)} \tag{6.43}$$

The velocity u_w is deduced from (6.40a). Then from the expression of the solid discharge (6.40b), the ratio α can be deduced

$$\alpha = \frac{q_s}{C_s h_s u_w} \tag{6.44}$$

Finally, the friction coefficient $C_{f,s}$ can be isolated in expression (6.42a), where (6.41) and (6.42b) have been substituted.

$$C_{f,s} = \frac{\tau_s}{\alpha^2 \rho_s' |u_w| \, u_w} = \frac{\tau_b}{\alpha^2 \rho_s' |u_w| \, u_w} \tag{6.45}$$

The obtained calibration value for the friction coefficient $C_{f,s}$ is identical to the one obtained when no link between the velocity in each layer is imposed (6.14). Even if the shear stress applied on the transport layer by the water layer and the corresponding friction coefficient $C_{f,w}$ are not necessary, they can be deduced. The shear stress τ_{ws} is deduced from (2.80) and then the coefficient $C_{f,w}$ is deduced from the definition of the shear stress τ_{ws} depending on the ratio α.

$$C_{f,w} = \frac{\tau_w}{\rho_w (1-\alpha)^2 \, |u_w| \, u_w} \tag{6.46}$$

which corresponds to the calibration value provided by (6.13). The ratio α is linked to the friction coefficients, an approximated relation is given by (6.26).

6.8. Preliminary experiments

In the context of their diploma work, Dubois and Jonckheere (2006) carried out experiments under uniform flow conditions, with the set-up described in chapter 5. The experiments are quite close from those realised by Armanini et al. (2005), but limited to sheet-flow, corresponding to bed-load transport. The aim of these experiments is to compare the experimental and the numerical predictions concerning the depth and the velocity of the transport layer. The experiment starts with a bed-slope lower than the equilibrium bed-slope corresponding to the liquid and solid discharge imposed at the upstream end of the flume. Then, an aggradation process is induced until the equilibrium slope is reached. The experiment was carried out for various liquid and solid discharges. Once the equilibrium is reached, the depth and the velocity of the transport layer are measured using digital imagery techniques. The transport layer depth is deduced from the position of the interfaces between the different layers using the method developed by

Spinewine and Zech (2002). The velocity profiles in the transport layer were obtained by tracking sediments using the Voronoï imaging methods described in Capart et al. (2002). One of the results from the experimental campaign indicates that the velocity profile in the transport layer is linear, as previously experimented by Spinewine (2005) in the case of dam-break flows. Unfortunately, the data are not presented here due to the discrepancy of the experimental measurements. Indeed, this experiment, which appears to be quite simple at first sight, reveals to be difficult to realise. It is not obvious to check whether the equilibrium conditions are reached or not. Some of the measurements were taken when the equilibrium conditions were not yet reached. Moreover, the presence of antidunes and saltation makes the results more complicated to interpret. In addition, the particle tracking, even if operational, is more difficult to apply when the particles are grains of sand in a transport layer. A new experimental campaign, more accurate, should be realised in the future.

6.9. Conclusions

The purpose of this chapter was to check if the two-layer model agrees with common approaches in the simple case of uniform flow. By comparison between classical and two-layer approaches, a calibration of the friction parameter was proposed. Models based on different assumptions were compared. Assuming different velocities in the water and the transport layer, and different sediment concentrations in the transport layer and in the fixed bed (Spinewine, 2002) is in agreement to several of well-known solid transport formulae. When the concentrations in the bed and in the transport layer are assumed to be the same (Capart and Young, 2002), the estimation of the solid discharge does not seem worse, but the thickness of the transport layer is less close to reality. Under the restrictive assumption of a constant velocity ratio between the two-layers, the good match with common solid transport formulae is conserved. Nevertheless, when the velocity is considered the same in both layers (Capart, 2000), the agreement disappears, and another formulation of the shear stresses along the interfaces should be proposed. Future experiments under uniform-flow conditions should allow to evaluate the accuracy of the transport layer thickness and the sediment velocity obtained with the two-concentration two-layer model.